
Learning to Disentangle Robust and Vulnerable Features for Adversarial Detection

Byunggil Joe
KAIST
cp4419@kaist.ac.kr

Sung Ju Hwang
KAIST
sjhwang82@kaist.ac.kr

Insik Shin
KAIST
insik.shin@kaist.ac.kr

Abstract

Although deep neural networks have shown promising performances on various tasks, even achieving human-level performance on some, they are shown to be susceptible to incorrect predictions even with imperceptibly small perturbations to an input. There exists a large number of previous works which proposed to defend against such adversarial attacks either by robust inference or detection of adversarial inputs. Yet, most of them cannot effectively defend against whitebox attacks where an adversary has a knowledge of the model and defense. More importantly, they do not provide a convincing reason why the generated adversarial inputs successfully fool the target models. To address these shortcomings of the existing approaches, we hypothesize that the adversarial inputs are tied to *latent* features that are susceptible to adversarial perturbation, which we call *vulnerable* features. Then based on this intuition, we propose a minimax game formulation to disentangle the latent features of each instance into robust and vulnerable ones, using variational autoencoders with two latent spaces. We thoroughly validate our model for both blackbox and whitebox attacks on MNIST, Fashion MNIST5, and Cat & Dog datasets, whose results show that the adversarial inputs cannot bypass our detector without changing its semantics, in which case the attack has failed.

1 Introduction

Although deep neural networks have achieved impressive performances on many tasks, sometimes even surpassing human performance, researchers have found that they could be easily fooled by even slight perturbations of inputs. Adversarial examples, which are deliberately generated to change the output without inducing semantic changes in the perspective of human perception [1, 2], can sometimes bring down the accuracy of the model to zero percent. Many of previous work try to solve this problem in the forms of robust inference [3, 4, 5, 6, 7, 8], which aims to obtain correct results even with the adversarial inputs, or by detecting adversarial inputs [9, 10, 11, 12, 13, 14, 15].

However most of previous works do not work properly in whitebox attack scenarios where the adversary has the same knowledge as a defender. Most of the past defenses which at a time successfully defended against adversarial attacks were later broken. For example, adversarial defenses leveraging randomness, obfuscated gradients, input denoising, and neuron activations which were once deemed as robust, were later broken with sophisticated whitebox attacks such as expectation over transformation or backward pass differentiable approximation [16, 17].

We hypothesize that the malfunctions of the previous defenses are caused by the existence of features that are more susceptible to adversarial perturbations, which misguide the model to make incorrect predictions. Such a concept of vulnerable features has been addressed in a few existing works [18, 19]. These approaches define vulnerability of the *input features* either based on the human perception, based on the amount of perturbation at the network output, or correlation with the label. Yet, our hypothesis has a different perspective of vulnerability/robustness in that we assume that there exists

a latent feature space where adversarial inputs to a label form a common latent distribution. That is, vulnerable and robust features by our definition are not input features, but rather *latent features* residing in hypothetical spaces. While vulnerability/robustness of features are assumed as given and fixed in the existing work, this redefinition allows us to explicitly *learn* to disentangle features into robust and vulnerable features by learning their feature spaces.

Toward this goal, we propose a variational autoencoder with two latent feature spaces, for robust and vulnerable features respectively. Then, we train this model using a two-player mini-max game, where the adversary tries to maximize the probability that the adversarially perturbed instances are in the robust feature space, and the defender tries to minimize this probability. This procedure of *learning* to disentangle robust and vulnerable features further allows us to *detect* features based on their likelihood of the feature belonging to either of the two feature categories (see Figure 1).

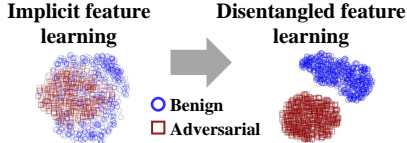


Figure 1: Latent spaces of features

We validate our model on multiple datasets, namely MNIST [20], Fashion MNIST5 [21], and Cat & Dog [22], and show that the attacks cannot bypass our detector without incurring semantic changes to the input images, in which the attack has failed.

Our contributions can be summarized as follows:

1. We empirically show that adversarial attacks are negative side effects of *vulnerable features*, which is the byproduct of *implicit representation learning* algorithms.
2. From the above empirical observation, we hypothesize that different adversarial inputs to a label form a common latent distribution.
3. Based on this hypothesis, we propose a new defense mechanism based on variational autoencoders with two latent spaces, and a two-player mini-max game to learn the two latent spaces, for robust and vulnerable features each, and use it as an adversarial input detector.
4. We conduct blackbox and whitebox attacks to our detector and show that adversarial examples cannot bypass it without inducing semantic changes, which means attack failure.

2 Related work

After revealing severe defects of neural networks against adversarial inputs[1, 2], researchers have found more sophisticated attacks to fool the neural networks[2, 4, 23, 24, 25, 26]. On the other side, many researchers have tried to propose a defense mechanism against such attacks as a form of robust prediction [3, 4, 5, 6, 7, 8] or detector of adversarial inputs [9, 10, 11, 12, 13, 14, 15]. Many of them rely on randomness, obfuscated gradients, or distribution of neuron activations, which are known to malfunction under adaptive whitebox attacks [16, 17]. Some of previous works studied root causes of this intriguing defects. Goodfellow et al.[2] suggest there should be vulnerability in benign input distributions with an interpretation of deep neural networks as linear classifiers. Tsipras et al.[18] further propose a dichotomy of robust feature and non-robust feature. They analyze the intrinsic trade-off between robustness and accuracy. Concurrent to this work, Ilyas et al.[19] find that non-robust features suffice for achieving good accuracy on benign inputs. They also provide a theoretical framework to analyze the non-robust features. On the other hand, we provide a hypothesis about *latent distributions of vulnerable features*, and disentangle vulnerable latent space from the entire latent feature space under adaptive whitebox attacks.

3 Background and Motivational Experiment

Premise. The key premise of our proposed framework is that standard neural-network classifiers implicitly learn two types of features: *robust* and *vulnerable* features. The robust features, in an intuitive sense, correspond to signals that make semantic sense to humans, which may describe texture, colors, local shapes or patches in image domain. The vulnerable features are considered as imperceptible to human senses but are leveraged by models for prediction since they help lowering the training loss. We posit that adversarial attacks exploit vulnerable features to imperceptibly perturb inputs that induce erroneous prediction.

Notation. We now present notations used throughout this paper. Firstly, $x \in \mathbb{R}^d$ is an input in d dimensions. We distinguish x between benign input x_b and adversarial input $x_a = x_b + \delta$, where $\delta \in S = \{\delta \mid \|\delta\|_p < \epsilon\}$. Typical p is one of 0, 1, 2, and ∞ . We use an ordered set X with matching subscripts b and a to indicate a set of x_b and x_a and with superscript c to indicate label c . Given an input x_b , the true label of x_b is y_b , and y_a is an inaccurate (misled) label of corresponding x_a . Y_b and Y_a are ordered sets of labels of x_b and x_a that have the same indice in X_b and X_a . The number of unique labels in classification is N . We denote a dataset as a pair (X, Y) . P_r^c and P_v^c are the probability density functions of robust features and vulnerable features respectively for the inputs of label c . θ^c is a set of model parameters of a variational autoencoder for label c (i.e., VAE^c).

Attack methods. We briefly explain representative attack methods used in this paper.

Fast Gradient Sign Method (FGSM) is an one step method proposed by Goodfellow et al. [2]. $L(x, y)$ is a training loss. The attack takes sign of $\nabla L(x, y)$ and perturbs the x with a size parameter ϵ to increase $L(x, y)$, resulting in an unexpected result.

$$x_a = x + \epsilon \cdot \text{sign}(\nabla L(x, y))$$

Projected Gradient Decent (PGD) is an iterative version of the FGSM attack with random start [4]. To generate x_a^{t+1} , the attack perturbs x_a^t with a step size parameter α based on the sign of $\nabla L(x_a^t, y)$. It limits its search space in the input space of $x + S$, which is implemented as a clipping function with a L_∞ bound. It can initialize the attack, adding uniform noise to an original image, $x_a^0 = x + U(S)$.

$$x_a^{t+1} = \prod_{x+S} (x_a^t + \alpha \cdot \text{sign}(\nabla L(x_a^t, y)))$$

Momentum Iterative Method (MIM) introduces concept of momentum to the PGD attack [23]. Instead of directly updating x_a^t from $\nabla L(x_a^t, y)$, it applies previous g^t value with decay factor μ to g^{t+1} . Then it updates x_a^{t+1} with the sign of g^{t+1} and the step size α , while limiting search space in $x + S$.

$$g^{t+1} = \mu \cdot g^t + \frac{\nabla L(x_a^t, y)}{\|\nabla L(x_a^t, y)\|_1}, \quad x_a^{t+1} = \prod_{x+S} (x_a^t + \alpha \cdot \text{sign}(g^{t+1}))$$

Carlini & Wagner Method (CW-L2) [24] introduces w and searches adversarial inputs on the w space, because it relaxes discontinuous property at the minimum and maximum input values. To minimize the distortion of adversarial inputs, it incorporates a L_2 loss term, $\|\frac{1}{2}(\tanh(w) + 1) - x\|_2^2$. It defines a function $f(x')$ to induce miss-classification, where $Z(x')_i$ is the logit value of label i right before a softmax layer, and t is a label of the original input x . The κ is for larger differences in logit values, resulting in high confidence. It balances between L_2 loss and $f(x')$ loss in a binary search of c .

$$\min_w \|\frac{1}{2}(\tanh(w)+1)-x\|_2^2 + c \cdot f(\tanh(w)+1), \quad f(x') = \max(\max(Z(x')_i : i \neq t) - Z(x')_t, -\kappa)$$

3.1 Vulnerability of Implicit Feature Learning

By showing that the vulnerable features are prevalent in benign datasets (X_b, Y_b) , we validate our argument that the implicit learning algorithms may lead models to learn vulnerable features that could be exploited by an adversary, without explicit regularizations to prevent learning of them. We now provide an evidence in support of this, where a benign dataset (X_b, Y_b) can be classified with good accuracy by a classifier F_v which is trained with a dataset (X_v, Y_v) only containing vulnerable features.

The basic idea to construct (X_v, Y_v) for F_v is to leverage a dataset of adversarial inputs (X_a, Y_a) that an arbitrary attack A generates, to fool a classifier F_p pre-trained with (X_b, Y_b) , where Y_a is a set of incorrect labels. The set of adversarial inputs X_a cause F to make erroneous prediction toward a target label y . That is, each X_a contains a set of vulnerable features that F_p learned to identify y , because the features do not contain any semantically meaningful features of y (see Figure 2). Based on this reasoning, we construct (X_v, Y_v) by attacking F_p and accumulating a set of X_a with the inaccurate labels Y_a . For clarity, (X_v, Y_v) should not contain robust features; it should not include benign inputs and should not allow large distortions that could change the semantics of the inputs.

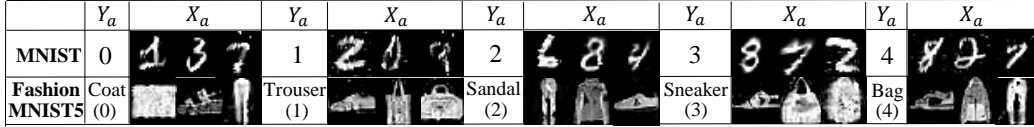


Figure 2: Examples of vulnerable feature dataset (X_v, Y_v) generated by the CW-L2_d attack

Table 1: Performance of a classifier F_v trained only with vulnerable feature dataset (X_v, Y_v)

	MNIST				Fashion MNIST5			
	FGSM_d	PGD_d	MIM_d	CW-L2_d	FGSM_d	PGD_d	MIM_d	CW-L2_d
Test X_b accuracy	0.37	0.85	0.92	0.98	0.53	0.71	0.78	0.78
Test X_v accuracy	0.54	0.81	0.73	0.96	1.0	0.95	0.93	1.0
# of iterations	2	7	30	30	3	30	30	30
D loss term of A^1	$-100D(x)$	$-10D(x)$	$-2D(x)$	$0.5D(x)$	$-10D(x)$	$-10D(x)$	$-1D(x)$	$0.5D(x)$

To make the accumulation process efficient, we introduce a discriminator D which learns the vulnerable features in (X_v, Y_v) and prevents the attack A from re-exploiting the vulnerable features that has already learned. The attack A should then bypass D , which is only possible with exploiting a new set of vulnerable features. After a pre-determined number of iterations for accumulation, we train F_v with (X_v, Y_v) and measure the performance of F_v on (X_b, Y_b) and test datasets (X'_v, Y'_v) .

We conduct this experiment ² with two datasets, MNIST and Fashion MNIST5. In the case of Fashion MNIST5, we use a subset of Fashion MNIST [21] which are "Coat (0)", "Trouser (1)", "Sandal (2)", "Sneaker (3)", and "Bag (4)". Figure 2 illustrates vulnerable feature datasets (X_v, Y_v) generated by A . We can see that X_v describes a completely different visual object classes from Y_v , as X_v is comprised of only the vulnerable features. For more details of the experiment, see Table A.1 in **supplementary file**.

We use four representative attacks, including FGSM_d, PGD_d, MIM_d, and CW-L2_d, where "_d" indicates that each individual base attack is adapted to bypass D with an additional attack objective. Table 1 summarizes the performance of F_v . Interestingly, the results show that it is possible to achieve high accuracy of up to 0.98 (MNIST) and 0.78 (Fashion MNIST5) on (X_b, Y_b) , even though they are trained with (X_v, Y_v) . We note that F_v also achieves high accuracy on test datasets (X'_v, Y'_v) , which are unseen in the training phase.

From the above experiments, we can draw the following two conclusions:

- High accuracy on (X_b, Y_b) : Vulnerable features are prevalent in (X_b, Y_b) , and we need new training algorithms that are able to distinguish vulnerable and robust features for robustness.
- High accuracy on (X'_v, Y'_v) : (X_v, Y_v) must share some high-level features in common, although they may be imperceptible to humans. Based on this observation, we hypothesize that the adversarial inputs X_v of the same label Y_v exist in the common latent distribution.

4 Approach

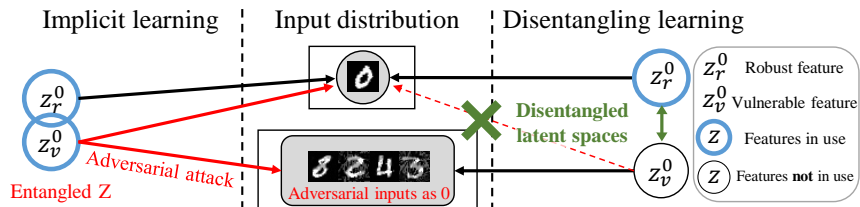


Figure 3: Implicit vs. disentangling learning in latent feature spaces (label 0 on MNIST)

⁰The sign of D loss depends whether an attack uses gradient descent(+) or ascent(-).

²It is worth noting that a similar experiment [19] was conducted independently at the same time. A key difference is that the experiment in [19] is designed to construct *non-robust* (vulnerable) input datasets while our experiment aims to construct a common latent distribution of a maximal set of vulnerable features with D .

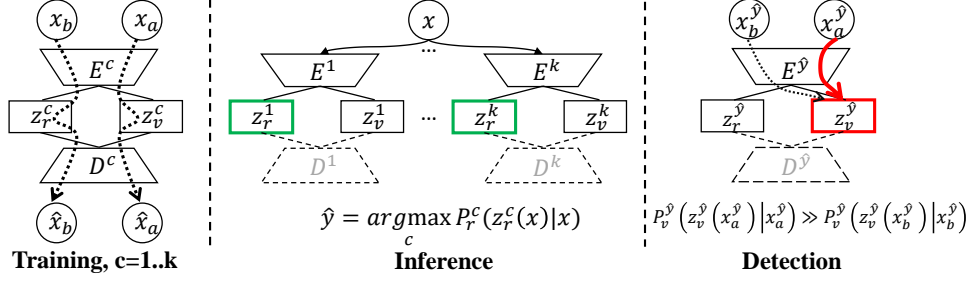


Figure 4: Proposed network architecture for the disentangling learning

Based on the hypothesis that vulnerable features make up a common latent distribution for each label, we propose a new learning algorithm to recognize and disentangle a latent space of the vulnerable features from distributions of the all features. Figure 3 shows the difference from an implicit algorithm (left) that learns latent features z without such distinction.

Specifically, we propose a variational autoencoder with two latent feature spaces z_r and z_v respectively for robust and vulnerable features. We regularize z_r and z_v not to estimate distributions of adversarial and benign inputs respectively, in addition to an original objective of the variational autoencoder, as a mini-max game. As the training converges, z_r gets close to a distribution of robust features, and z_v represents a distribution of vulnerable features. Then the z_v could be used to detect adversarial inputs, since they will form a distinct distribution in z_v that separates them from benign inputs.

4.1 Mini-max game

A key idea of our proposed training can be represented as two-player mini-max game between a defender and an adversary on the two probability distributions of the robust features P_r^c and the vulnerable features P_v^c of each label c . The defender seeks to detect an adversarial attack on an input x by checking if $P_v^c(x)$ is higher than a threshold, and the adversary aims to maliciously perturb the input x while compromising the detection.

$$\min_{\theta^c} \max_{\delta \in S} \log P_r^c(x + \delta) + \log(1 - P_v^c(x + \delta))$$

In the beginning, P_r^c is initialized to reflect the distribution of all the robust and vulnerable features, but P_v^c does not represent a feature. Each player alternately plays the game. In the adversary's turn, the adversary perturbs x with $\delta \in S$, in order to maximize P_r^c but minimize P_v^c to compromise the defender. In the next turn, the defender controls the model parameter θ^c to perform the opposite, aiming to collect all the vulnerable features that have been exploited by the adversary and segregate them into the distribution of P_v^c . If the defender successfully detects all the vulnerable features, then the defender wins the game. Otherwise, the adversary wins. However, since the set of vulnerable features is finite with the finite size of θ^c , the defender with a proper detection strategy will eventually win the game, after a sufficient number of turns.

4.2 Network architecture

To embed the proposed mini-max game in a training process, we suggest a network architecture described in Figure 4. For each label c , we have a variational autoencoder VAE^c[27] that consists of an encoder $E^c(x)$ and a decoder $D^c(x)$. Instead of one type of latent variables, $E^c(x)$ samples two types of latent variables z_r^c and z_v^c for each of benign and adversarial inputs of the label c . We denote $E^c(x) = E_r^c(x) \cdot E_v^c(x) = z_r^c(x) \cdot z_v^c(x)$ for simplicity. $D^c(z)$ generates \hat{x} for any given z , where z is either $z_r^c(x)$ or $z_v^c(x)$ depending on whether x is x_b or x_a . The information is given in the training process as a flag, and $D^c(x)$ can selectively take $z_r^c(x_b)$ or $z_v^c(x_a)$ based on the flag.

For classification, we integrate the VAE^cs into a classifier $F(x)$. Given an input x , $F(x)$ estimates probabilities of x on P_r^c of each VAE^c, and returns an index of the highest probability as the predicted label \hat{y} . This process can be denoted as $\hat{y} = F(x) = \arg \max_c P_r^c(z_r^c(x)|x)$. For the detection of an adversarial input x_a , we utilize the probability of x_a on $P_v^{\hat{y}}$ relatively compared to the values of $X_b^{\hat{y}}$, given the predicted label $\hat{y} = F(x_a)$. Specifically, we detect if $P_v^{\hat{y}}(z_v^{\hat{y}}(x)|x) \gg P_v^{\hat{y}}(z_v^{\hat{y}}(x_i)|x_i)$, where $x_i \in X_b^{\hat{y}}$.

4.3 Training the network

We train each VAE^c with the loss l^c . We design l^c based on an evidence lower bound of $\log P_r^c(x_b) + \log P_v^c(x_a)$ with two regularization terms, which penalize errors in variational inference. Specifically, when erroneous estimates happen, that is, when E_r^c assigns x_a with high probability or E_v^c assigns x_b with high probability, VAE^c is penalized and encouraged to distinguish between the robust features of x_b and the vulnerable features in x_a . We provide the detailed derivation of l^c in Section A.2 of the **supplementary file**. The final form of l^c is as follows, where $\mu_i(z)$ selects the i -th mean element of z , and $\sigma_i(z)$ selects the i -th standard deviation element of z from reparameterization.

$$\begin{aligned}
 l^c &= \|x_b - D^c(E_r^c(x_b))\|^2 + \|x_a - D^c(E_v^c(x_a))\|^2 && \text{(Reconstruction loss)} \\
 &- \frac{1}{2}\alpha \sum_i^{|E_r^c(x_b)|} (1 + \log(\sigma_i^2(E_r^c(x_b))) - \mu_i^2(E_r^c(x_b)) - \sigma_i^2(E_r^c(x_b))) && \text{(KL divergence for } z_r^c) \\
 &- \frac{1}{2}\alpha \sum_i^{|E_v^c(x_a)|} (1 + \log(\sigma_i^2(E_v^c(x_a))) - \mu_i^2(E_v^c(x_a)) - \sigma_i^2(E_v^c(x_a))) && \text{(KL divergence for } z_v^c) \\
 &- \beta \{ \log(1 - \mathcal{N}(E_r^c(x_a)|0, I)) + \log(1 - \mathcal{N}(E_v^c(x_b)|0, I)) \} && \text{(} z^c \text{ error penalty)}
 \end{aligned}$$

We choose the pixel-wise mean squared error (MSE) for the first two terms as reconstruction errors, and the standard normal distribution $\mathcal{N}(0, I)$ as priors for P_r^c and P_v^c . We also introduce constants α and β , respectively, for the KL divergence terms and the loss terms of variational inference for a practical purpose.

Before we train VAE^c with l^c we should incorporate the knowledge of our defense mechanism to the existing attacks, considering the whitebox attack model. Given an attack loss l_{attack} of an arbitrary attack A , we linearly combine a term $l_{pass} = \max(0, P_v^{\hat{y}}(z_v^{\hat{y}}(x_a)|x_a) - E_{x^i \in X_b^{\hat{y}}}[P_v^{\hat{y}}(z_v^{\hat{y}}(x^i)|x^i)])$ to bypass our detector with a coefficient γ . As a result we get $l_{adapt_attack} = l_{attack} \pm \gamma l_{pass}$. We also introduce a binary search to find the proper γ in a similar way to the CW-L2 attack. We modify all the attacks in this paper. We denote an attack with "_W", if the attack is modified to work on the whitebox model. The sign of the γL_v term depends on whether the attack is based on gradient descent (+), or ascent (-).

Algorithm 1 describes our training algorithm. It is an iterative process, where at each iteration A_W attacks VAE^c to exploit vulnerable features in P_r^c , and the VAE^c corrects the distribution P_r^c and P_v^c with θ^c to identify vulnerable features found in each iteration. We should only attack $X_b - X_b^c$, in order to prevent the inclusion of robust features in P_v^c . The training ends when A_W can not find adversarial inputs that could bypass the detector.

Algorithm 1: Training process of VAE^c

```

 $X_v^c \leftarrow \phi$  : Set of adversarial inputs to label  $c$ 
 $A\_W$  : An adapted whitebox attack
while  $A\_W$  successes to bypass do
   $X_v^c \leftarrow X_v^c \cup A\_W(X_b - X_b^c, \text{VAE}^c)$ 
  TRAIN VAEc to distinguish  $X_b^c$  and  $X_v^c$ 
  maximizing  $l^c$  with  $\theta^c$ 
end while

```

5 Experiment

We evaluate our defense mechanism under both blackbox and whitebox attacks, trained with MIM_W and CW-L2_W. In the blackbox setting, we evaluate how precisely our detector filters out adversarial inputs by measuring AUC scores. In the whitebox setting, we first quantitatively evaluate attack success ratio and qualitatively analyze whether successful adversarial inputs induce semantic changes.

Table 2: (X_b, Y_b) accuracy of models

	MIM_W	CW-L2_W	No defense
MNIST	0.97	0.98	0.99
Fashion MNIST5	0.98	0.98	0.99
Cat & Dog	0.96	0.96	0.99

Baseline. We choose Gong et al. [11] as a baseline for comparison, which also leverages adversarial inputs to train an auxiliary classifier for detecting adversarial inputs. Note that Gong et al. does not incorporate adaptive attacks in their approach, although we denote it with the same notation (e.g., MNIST, A=PGD_W).

Table 3: AUC scores of blackbox attack detection. Our approach (left) remains more generalized over various attacks compared to the baseline (right)

	MNIST		Fashion MNIST5	
	MIM_W	CW-L2_W	MIM_W	CW-L2_W
FGSM	0.99 / 0.99	0.98 / 0.99	0.98 / 0.99	0.99 / 0.97
PGD	0.99 / 0.96	0.99 / 0.99	0.97 / 0.79	0.99 / 0.96
MIM	0.99 / 0.90	0.99 / 0.98	0.98 / 0.92	0.99 / 0.97
CW	0.97 / 0.64	0.97 / 0.96	0.96 / 0.64	0.97 / 0.95

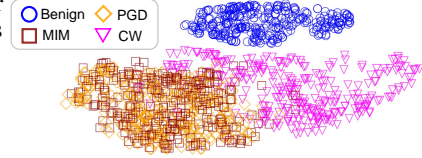


Figure 5: Disentangled latent distributions of robust and vulnerable features (blue x_b vs. others x_a), on MNIST, A=MIM_W VAE^{c=3}.

Attacks. Our attacks are based on the publicly available implementations [28, 29], and the whitebox attacks are adapted to bypass our detection mechanism. All adversarial inputs are generated from a separate test dataset, in an untargeted way.

Datasets. We evaluate our detector on the MNIST [20], Fashion MNIST5 [21], and Cat & Dog [22] datasets. In the case of the Cat & Dog dataset, we collect total 2028 frontal faces of cats and dogs, and resize it into 64 x 64 x 1 with a single channel.

We first show that our defense methods achieve a level of accuracy similar to those without defense mechanisms (see Table 2). Additional information including training parameters and details of the attacks are described in Section A.3 of the **supplementary file**.

5.1 Blackbox substitute model attack

In the blackbox setting, the adversary has no information regarding our defense mechanism, but we assume that the adversary has the same datasets as a defender. The adversary builds its own standard substitute classifier F_s , and generates a group of adversarial inputs x_a with an attack A to fool F_s . After that, the adversary attacks F with x_a , and the defender detects x_a based on the values of $P_v^{\hat{y}}(z_v^{\hat{y}}(x_a)|x_a)$ where $\hat{y} = F(x_a)$. The blackbox substitute model attacks are possible exploiting the transferability [2, 30, 31, 32, 33] of x_a over classifiers trained with similar datasets.

Table 3 shows AUC scores for detection results, where each cell compares ours (left) with the baseline (right) for each individual attack while our defense approaches achieve 0.98 on average and perform better than the baseline by up to 0.33. We attribute the success of our model to its ability to disentangle the distribution of the vulnerable features of x_a into z_v from the distribution of whole features. To see if the features are actually disentangled, we visualize z^c with t-SNE [34] in Figure 5. It shows clear separation between $z_v^c(x_b^c)$ and $z_v^c(x_a^c)$ as we expected. We conclude that the transferability between the models is reduced by disentangling the vulnerable features which the adversary might exploit for F_s found in benign datasets.

5.2 Whitebox attack

Whitebox attacks are difficult to defend because the adversary has exactly the same knowledge as the defender, which could be exploited in order to fool the defender. For clear analysis, we define a set of success conditions C of the adversary when an inference label of x_a is $\hat{y} = F(x_a)$, as follows:

- C1 Low probability on vulnerable features to bypass the detector: $P_v^{\hat{y}}(x_a) < E[P_v^{\hat{y}}(x_b^{\hat{y}})]$.
- C2 High probability on robust features to convince the defender: $P_r^{\hat{y}}(x_a) > E[P_r^{\hat{y}}(x_b^{\hat{y}})]$.
- C3 Semantic meaning of the original input should be retained.

For $C1$ and $C2$, Figure 6 plots attack success ratios along the L_∞ distortion on MNIST and Fashion MNIST5. As L_∞ increases, the success ratio also increases except FGSM_W. Our defense shows gradual slope compared to the baseline. Table 4 shows the whitebox attack result of CW-L2_W with minimized distortions in a binary search. CW-L2_W achieves average success ratio of 0.30 and 0.19 with L_2 distortion³ of 46.66 and 40.5 for MNIST and Fashion MNIST5, respectively.

Table 4: Result of CW-L2_W attack

A	MNIST		Fashion MNIST5	
	MIM_W	CW-L2_W	MIM_W	CW-L2_W
Ratio	0.32	0.28	0.18	0.19
Mean L_2	45.08	48.25	43.34	37.66

³The L_2 distortion is calculated as $\|\delta\|_2/\sqrt{d}$ in $[0, 255]$ input range.

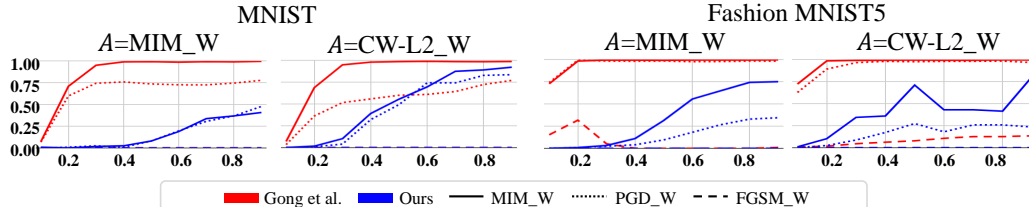


Figure 6: Success ratio of whitebox attacks along the L_∞ distortion (according to C1 & C2)

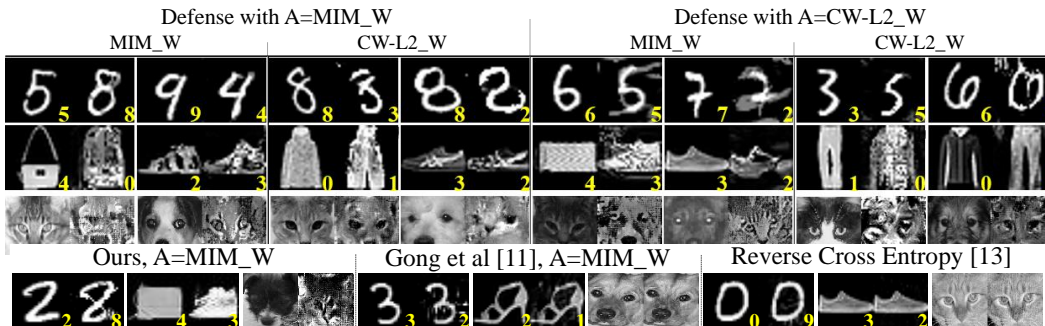


Figure 8: Semantic comparison to baselines[11, 13] under the CW-L2_W attack; the attack yields larger semantic changes on our approach compared to the baselines⁴

Regarding C3, Figure 7 compares the visual differences between each pair of a benign image (left) and an adversarial image (right). The predicted label for each image is shown in yellow, in the bottom right corner. We choose $L_\infty = 0.5$ as a reference distortion value for the MIM_W attacks. We can clearly observe the semantic changes on the adversarial images. We additionally evaluate our defense mechanism on a Cat & Dog dataset. It also shows the semantics changed between the labels ($L_\infty = 0.3$). Some lines are appeared or disappeared in MNIST rather than noisy dots, and sneakers turn into sandals with similar styles such as overall shape or pattern. In the case of Cat & Dog dataset, features of dogs are appearing in the adversarial inputs generated from cats as big noses and long spouts, while the brightness of the fur, or angles of faces seem to be preserved. Figure 8 show adversarial perturbations from the attacks result in clear semantic changes with our approach compared to other baselines. We provide more results obtained with various L_∞ including the PGD_W attack in Section A.4 of the **supplementary file**. From the result we conclude our approach successfully distinguishes vulnerable features from whole features compared to the baseline. Furthermore, considering the semantic changes of adversarial inputs, we conclude that the robust features estimated in z_r are well-aligned with human perception.

6 Conclusion

In this work, we hypothesize about the latent feature space for adversarial inputs of a label and conjectured that feature space entanglement of vulnerable and robust features is the main reason of adversarial vulnerability of neural networks, and proposed to *learn* a space that disentangles the latent distributions of the vulnerable and robust features. Specifically, we trained a set of variational autoencoders for each label with two latent spaces, and trained them using a two-player mini-max game, which results in learning disentangled representations for robust and vulnerable features. We show that our approach successfully identifies the vulnerable features and also identifies sufficiently robust features in the whitebox attack scenario. However, we cannot guarantee that our approach is a panacea, and further research is required for the discovery of new attacks. We hope our work stimulates research toward more reliable and explainable machine learning.

⁴We found and corrected implementation errors in the robustness evaluation of the reverse cross entropy [13], and we could bypass the detector in the adaptive whitebox attack. We confirmed it with an author of the paper.

References

- [1] C. Szegedy, J. Bruna, D. Erhan, and I. Goodfellow, “Intriguing properties of neural networks,” in *In International Conference on Learning Representations (ICLR)*. 2014.
- [2] I. J. Goodfellow, J. Shlens, and C. Szegedy, “Explaining and harnessing adversarial examples,” in *International Conference on Learning Representations (ICLR)*. 2015.
- [3] S. Gu and L. Rigazio, “Towards deep neural network architectures robust to adversarial examples,” in *International Conference on Learning Representations (ICLR) Workshops*. 2015.
- [4] A. Mađry, A. Makelov, L. Schmidt, D. Tsipras, and A. Vladu, “Towards Deep Learning Models Resistant to Adversarial Attacks,” in *International Conference on Learning Representations (ICLR)*. 2018.
- [5] S. Zheng, Y. Song, T. Leung, and I. Goodfellow, “Improving the robustness of deep neural networks via stability training,” in *In The IEEE Conference on Computer Vision and Pattern Recognition (CVPR)*. 2016.
- [6] P. Samangouei, M. Kabkab, and R. Chellappa, “Defense-gan: Protecting classifiers against adversarial attacks using generative models,” 2018.
- [7] L. Schott, J. Rauber, M. Bethge, and W. Brendel, “Towards the first adversarially robust neural network model on mnist,” in *International Conference on Learning Representations (ICLR)*. 2019.
- [8] G. S. Dhillon, K. Azizzadenesheli, and Z. C. Lipton, “Towards the first adversarially robust neural network model on mnist,” in *International Conference on Learning Representations (ICLR)*. 2018.
- [9] S. Ma, Y. Liu, G. Tao, W.-c. Lee, and X. Zhang, “NIC : Detecting Adversarial Samples with Neural Network Invariant Checking,” in *Proceedings of the 2019 Annual Network and Distributed System Security Symposium (NDSS)*. 2019.
- [10] R. Feinman, R. R. Curtin, S. Shintre, and A. B. Gardner, “Detecting Adversarial Samples from Artifacts,”. [arXiv:arXiv:1703.00410v3](https://arxiv.org/abs/1703.00410v3).
- [11] Z. Gong, W. Wang, and W.-s. Ku, “Adversarial and Clean Data Are Not Twins,” 2017. [arXiv:arXiv:1704.04960v1](https://arxiv.org/abs/1704.04960v1).
- [12] K. Grosse, P. Manoharan, N. Papernot, M. Backes, and P. McDaniel, “On the (Statistical) Detection of Adversarial Examples,”. [arXiv:1702.06280v2](https://arxiv.org/abs/1702.06280v2).
- [13] T. Pang, C. Du, Y. Dong, and J. Zhu, “Towards Robust Detection of Adversarial Examples,” in *Conference on Neural Information Processing Systems (NIPS)*. 2018.
- [14] W. Xu, D. Evans, and Y. Qi, “Feature Squeezing : Detecting Adversarial Examples in Deep Neural Networks,” in *Proceedings of the 2018 Annual Network and Distributed System Security Symposium (NDSS)*. 2018.
- [15] J. Wang, G. Dong, J. Sun, X. Wang, and P. Zhang, “Adversarial Sample Detection for Deep Neural Network through Model Mutation Testing,” in *CoRR*. 2018. [arXiv:1812.05793v2](https://arxiv.org/abs/1812.05793v2).
- [16] A. Athalye, N. Carlini, and D. Wagner, “Obfuscated Gradients Give a False Sense of Security : Circumventing Defenses to Adversarial Examples,” [arXiv:1802.00420v4](https://arxiv.org/abs/1802.00420v4).
- [17] N. Carlini and D. Wagner, “Adversarial Examples Are Not Easily Detected : Bypassing Ten Detection Methods,” in *In Proceedings of the 10th ACM Workshop on Artificial Intelligence and Security*. 2017. [arXiv:1705.07263v2](https://arxiv.org/abs/1705.07263v2).
- [18] D. Tsipras, S. Santurkar, L. Engstrom, A. Turner, and A. Mađry, “Robustness May Be at Odds with Accuracy,” in *International Conference on Learning Representations (ICLR)*. 2018.
- [19] A. Ilyas, S. Santurkar, D. Tsipras, L. Engstrom, B. Tran, and A. Madry, “Adversarial examples are not bugs, they are features,” 2019.
- [20] Y. LeCun, L. Bottou, Y. Bengio, and P. Haffner, “Gradient-based learning applied to document recognition,” in *Proceedings of the IEEE*, 86(11):2278–2324. 1998.
- [21] H. Xiao, K. Rasul, and R. Vollgraf, “Fashion-mnist: a novel image dataset for benchmarking machine learning algorithms,” 2017.

- [22] “Kaggle cats and dogs dataset.”
<https://www.microsoft.com/en-us/download/details.aspx?id=54765>.
- [23] Y. Dong, F. Liao, T. Pang, H. Su, J. Zhu, X. Hu, and J. Li, “Boosting Adversarial Attacks with Momentum,” in *In Proceedings of the IEEE Conference on Computer Vision and Pattern Recognition (CVPR)*. 2018.
- [24] N. Carlini and D. Wagner, “Towards Evaluating the Robustness of Neural Networks,” in *IEEE Symposium on Security and Privacy*. 2017.
- [25] S. M. Moosavi-Dezfooli, A. Fawzi, and P. Frossard, “DeepFool: A Simple and Accurate Method to Fool Deep Neural Networks,” *Proceedings of the IEEE Computer Society Conference on Computer Vision and Pattern Recognition 2016-Decem* (2016) 2574–2582, arXiv:1511.04599v3.
- [26] P.-Y. Chen, Y. Sharma, H. Zhang, J. Yi, and C.-J. Hsieh, “EAD: Elastic-Net Attacks to Deep Neural Networks via Adversarial Examples,” in *In AAAI Conference on Artificial Intelligence*. 2018. arXiv:1709.04114. <http://arxiv.org/abs/1709.04114>.
- [27] D. P. Kingma and M. Welling, “Auto-Encoding Variational Bayes,” in *International Conference on Learning Representations (ICLR)*. 2013.
- [28] “Mnist adversarial examples challenge.”
https://github.com/MadryLab/mnist_challenge. Accessed: 2010-09-30.
- [29] N. Papernot, F. Faghri, N. Carlini, I. Goodfellow, R. Feinman, A. Kurakin, C. Xie, Y. Sharma, T. Brown, A. Roy, A. Matyasko, V. Behzadan, K. Hambardzumyan, Z. Zhang, Y.-L. Juang, Z. Li, R. Sheatsley, A. Garg, J. Uesato, W. Gierke, Y. Dong, D. Berthelot, P. Hendricks, J. Rauber, and R. Long, “Technical report on the cleverhans v2.1.0 adversarial examples library,” *arXiv preprint arXiv:1610.00768* (2018) .
- [30] Y. Liu, X. Chen, C. Liu, and D. Song, “Delving into transferable adversarial examples and black-box attacks,” in *International Conference on Learning Representations (ICLR)*. 2017.
- [31] A. Ilyas, L. Engstrom, A. Athalye, and J. Lin, “Black-box adversarial attacks with limited queries and information,” in *International Conference on Learning Representations (ICLR)*. 2018.
- [32] N. Narodytska and S. Prasad Kasiviswanathan, “Simple black-box adversarial perturbations for deep networks,” in *In The IEEE Conference on Computer Vision and Pattern Recognition (CVPR)*. 2017.
- [33] P.-Y. Chen, H. Zhang, Y. Sharma, J. Yi, and C.-J. Hsieh, “Zoo: Zeroth order optimization based black-box attacks to deep neural networks without training substitute models,” in *In Proceedings of the 10th ACM Workshop on Artificial Intelligence and Security (AISec)*. 2017.
- [34] G. H. Laurens van der Maaten, “Visualizing Data using t-SNE,” *Journal of Machine Learning Research* (2008) .
- [35] R. O. Duda, P. E. Hart, and D. G. Stork, *Pattern Classification*. 2000.

A Appendix

A.1 Additional information about the motivational experiment

We conducted the motivational experiments described in the Section 3.1 to demonstrate that the classifier F_v trained with a dataset (X_v, Y_v) only containing vulnerable features can achieve high accuracy on a benign dataset (X_b, Y_b) . Table 5 and Table 6 describe the model parameters and the attack parameters used in the experiments. Algorithm 2 details the process of creating (X_v, Y_v) with the discriminator D .

We use abbreviated notations in Table 5, and Table 6. The "c(x,y)" is a convolutional layer with ReLU activation. The x is size of a kernel, and the y is the number of kernels. "mp(x)" is a max pooling layer whose pooling size is x by x. The "d(x)" is a dense layer where x is the number of neurons. The "sm(x)" is a softmax layer with output dimension x. For the attack parameter, "e" is L_∞ epsilon and i is iteration of attacks. "ss" is a step size of perturbations. "df" is a decay factor for the MIM attack. "lr", "cf", "ic", "bs" are learning rate, confidence, initial coefficient for the miss-classification loss, and the number of binary search steps.

For the fashion MNIST5, we intentionally choose the subset of Fashion MNIST such as coat (0), trouser (1), sandal (2), sneaker (3), bag (4) for decreasing effect of inter-label robust features. For example, sneaker and ankle boot, coat and pull over are quite similar. By doing so, we could extract vulnerable features only for each label and get an accurate result.

We implement the discriminator D as a separate model with one dimension of sigmoid output. The D learns to distinguish benign inputs as 0, and adversarial inputs as 1. As a consequence, we can interpret the output value of D as a probability where an input x would be an adversarial input. In terms of the bypassing D for attacks, we linearly incorporate the output value of D in objective loss functions of the attacks. As the attacks minimizing the output probability of D , the attacks generate new x_a with new vulnerable features.

Table 5: Model parameters in the motivational experiment

Models	Parameters
MNIST, F_p	c(2,20) mp(2) c(2,50) mp(2) d(500) sm(10)
MNIST, F_v	c(5,20) mp(2) c(5,50) mp(2) d(256) sm(10)
Fashion MNIST5, F_p	c(5,20) mp(2) c(5,50) mp(2) d(500) sm(10)
Fashion MNIST5, F_v	c(5,20) mp(2) c(5,50) mp(2) d(256) sm(10)

Table 6: Attack parameters in the motivational experiment

	Blackbox substitute model attacks			
	FGSM	PGD	MIM	CW-L2
MNIST	e:0.3	e:0.3, i:90, ss:0.01	e:0.3, i:640, ss:0.01, df:0.3	i:160, lr:0.1, cf:3, ic:10, bs:1
Fashion MNIST5	e:0.3	e:0.4, i:90, ss:0.01	e:0.3, i:320, ss:0.001, df:0.3	i:160, lr:0.1, cf:3, ic:10, bs:1

A.2 Training loss derivation

To approximate and distinguish the latent variable distributions of z_r^c and z_v^c , we maximize $ELBO(L^c)$ for each VAE^c, where

$$L^c = L_E^c + L_I^c \tag{1}$$

L^c consists of two terms. The first one is an evidence term L_E^c indicating the probability of occurrence of x_b and x_a , where

$$L_E^c = \log P_r^c(x_b) + \log P_v^c(x_a) \tag{2}$$

Algorithm 2: Training process only with the vulnerable features X_v

(X_b, Y_b) : Given benign dataset
 $(X_v, Y_v) \leftarrow (\phi, \phi)$: Empty dataset for vulnerable features
 F, F' : Pre-trained and initialized model respectively with same input and output dimensions
 A : Arbitrary attack
 D : Discriminator between benign (0) and adversarial (1) inputs
while $i < limit$ **do**
 $X_v^i, Y_v^i \leftarrow A(X_b, Y_b, F, D)$
 $(X_v, Y_v) \leftarrow (X_v \cup X_v^i, Y_v \cup Y_v^i)$
 TRAIN D to distinguish X_b and X_v
end while
TRAIN F' with X_v and Y_v
PRINT accuracy of F' on X_b and Y_b

The second one is a loss term of variational inference which penalizes in the case of wrong variation inference to each distribution P_r^c and P_v^c . It can be expanded to incorporate latent variables z_r^c and z_v^c as follows.

$$\begin{aligned} L_I^c &= \log(1 - P_r^c(x_a)) + \log(1 - P_v^c(x_b)) \\ &= \log(1 - \sum_{z_r^c(x_a)} P_r^c(x_a) P_r^c(z_r^c(x_a)|x_a)) + \log(1 - \sum_{z_v^c(x_b)} P_v^c(x_b) P_v^c(z_v^c(x_b)|x_b)) \quad (3) \\ &= \log(1 - E[P_r^c(z_r^c(x_a)|x_a)]) + \log(1 - E[P_v^c(z_v^c(x_b)|x_b)]) \end{aligned}$$

Plugging typical ELBO expansion [27] of the L_E^c term, and the L_I^c term into the equation 1, we get following $ELBO(L^c)$.

$$\begin{aligned} L^c &\geq E[\log P_r^c(x_b|z_r^c(x_b))] + E[\log P_v^c(x_a|z_v^c(x_a))] \\ &\quad - KL[q_r^c(z_r^c(x_b)|x_b)||P_r^c(z_r^c(x_b))] - KL[q_v^c(z_v^c(x_a)|x_a)||P_v^c(z_v^c(x_a))] \quad (4) \\ &\quad + \log(1 - E[P_r^c(z_r^c(x_a)|x_a)]) + \log(1 - E[P_v^c(z_v^c(x_b)|x_b)]) \\ &= ELBO(L^c) \end{aligned}$$

$$\begin{aligned} l^c &= \|x_b - D^c(E_r^c(x_b))\|^2 + \|x_a - D^c(E_v^c(x_a))\|^2 \\ &\quad - \frac{1}{2}\alpha \sum_i^{|E_r^c(x_b)|} (1 + \log(\sigma_i^2(E_r^c(x_b))) - \mu_i^2(E_r^c(x_b)) - \sigma_i^2(E_r^c(x_b))) \quad (5) \\ &\quad - \frac{1}{2}\alpha \sum_i^{|E_v^c(x_a)|} (1 + \log(\sigma_i^2(E_v^c(x_a))) - \mu_i^2(E_v^c(x_a)) - \sigma_i^2(E_v^c(x_a))) \\ &\quad - \beta \{ \log(1 - \mathcal{N}(E_r^c(x_a)|0, I)) + \log(1 - \mathcal{N}(E_v^c(x_b)|0, I)) \} \end{aligned}$$

We choose the pixel-wise mean squared error (MSE) for the first two terms as reconstruction errors, and the standard normal distribution $\mathcal{N}(0, I)$ as priors for P_r^c and P_v^c . We also introduce constants α and β , respectively, for the KL divergence terms and the loss terms of variational inference for a practical purpose.

A.3 Training and attack parameters

We use abbreviated notations in Table 7 as like in Table 5 In addition to that the "z(x,y)" is a sampling layer for latent variables. The x and y are dimensions of z_r and z_v . We use $\alpha = 1$ and $\beta = 100$ in all trainings. For the label inference we choose the nearest mean classifier on P_r^c , because its linear property prevents the vanishing gradients problem which makes attacks fail but known to be penetrable.

A.4 Additional figures about the whitebox attacks

In this section, we qualitatively evaluate the performance of our proposed defense mechanism against whitebox attacks as a function of epsilon. Figures 9, 10, and 11 show the results of the PGD_W and



Figure 10: Whitebox attack changes semantics of inputs (Fashion MNIST)

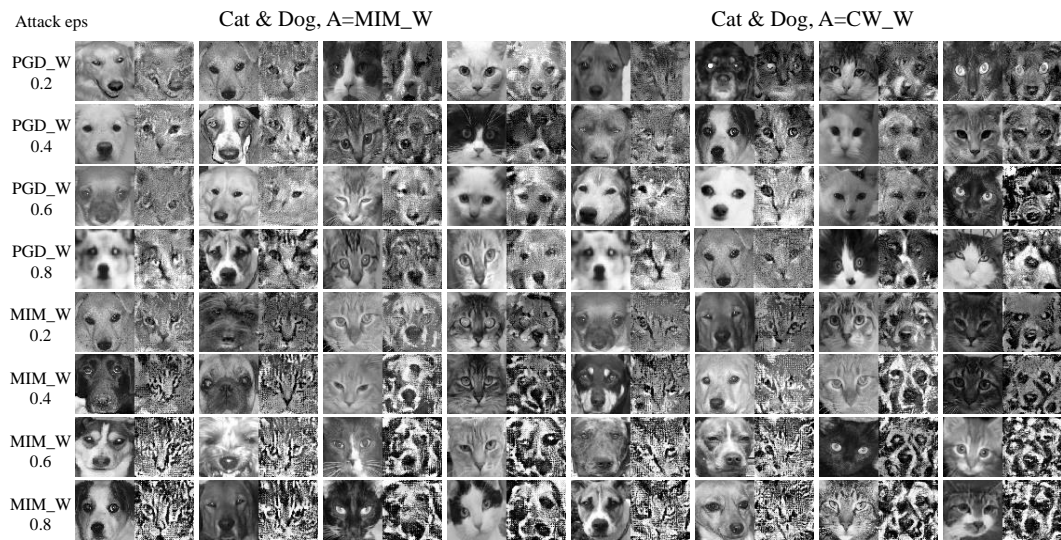


Figure 11: Whitebox attack changes semantics of inputs (Cat & Dog)

features) compared to the other datasets, and it is more difficult for attackers to detect them during perturbation.

In terms of the comparison of the state of the art, our defense mechanism shows clear semantic changes against the attacks. For example Gong et al.’s auxiliary classifier as a detector does not induce any robustness under adaptive whatbox attacks, and Reverse cross entropy which tries to impose non-maximal entropy in training phase, also does not work in whitebox attack unlike with the report in the paper. Actually it could not show significant robustness increase compared to the Gong et al.’s approach in terms of the amount of distortion and semantic changes (see Figure 13).

A.5 Experiment environments

We conduct our experiments on Ubuntu 16.04 machine with 4 GTX 1080 ti graphic cards and 64GB RAM installed. We build our experiments with tensorflow version 1.12.0, on python version 3.6.8.

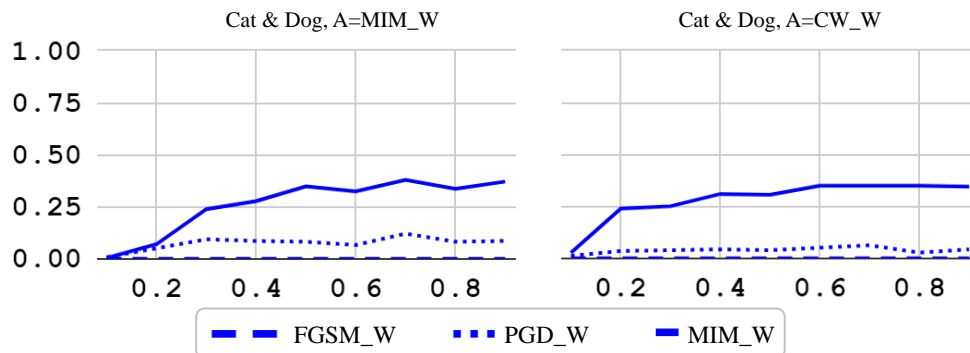


Figure 12: Whitebox attack success ratio along the L_∞ distortion (Cat & Dog).

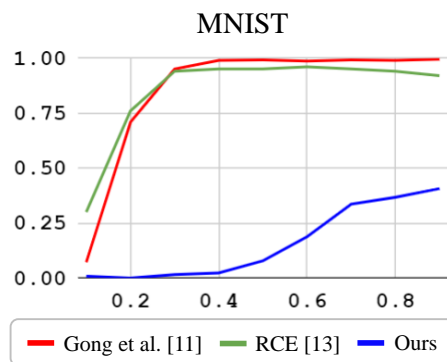


Figure 13: Baseline comparison on MIM_W whitebox attack success ratio (C1, C2) along the L_∞ distortion. Gong et al. and Ours are trained with MIM_W attack